Wake Flow Simulation of a Vertical Axis Wind Turbine Under the Influence of Wind Shear

IOP Conf. Series: Journal of Physics: Conf. Series **854** (2017) 012031 doi:10.1088/1742-6596/854/1/012031

Wake Flow Simulation of a Vertical Axis Wind Turbine Under the Influence of Wind Shear

Victor Mendoza and Anders Goude

Department of Engineering Sciences, Division of Electricity, Uppsala University, Uppsala 751 21, Sweden

E-mail: victor.mendoza@angstrom.uu.se

Abstract. The current trend of the wind energy industry aims for large scale turbines installed in wind farms. This brings a renewed interest in vertical axis wind turbines (VAWTs) since they have several advantages over the traditional Horizontal Axis Wind Tubines (HAWTs) for mitigating the new challenges. However, operating VAWTs are characterized by complex aerodynamics phenomena, presenting considerable challenges for modeling tools. An accurate and reliable simulation tool for predicting the interaction between the obtained wake of an operating VAWT and the flow in atmospheric open sites is fundamental for optimizing the design and location of wind energy facility projects. The present work studies the wake produced by a VAWT and how it is affected by the surface roughness of the terrain, without considering the effects of the ambient turbulence intensity. This study was carried out using an actuator line model (ALM), and it was implemented using the open-source CFD library OpenFOAM to solve the governing equations and to compute the resulting flow fields. An operational H-shaped VAWT model was tested, for which experimental activity has been performed at an open site north of Uppsala-Sweden. Different terrains with similar inflow velocities have been evaluated. Simulated velocity and vorticity of representative sections have been analyzed. Numerical results were validated using normal forces measurements, showing reasonable agreement.

1. Introduction

The amount of wind farms that are being built is increasing considerably, and it produces a relevant interest in the scientific community for the understanding of the interaction between the produced wake from the turbines and the atmospheric turbulent flow [1–5]. Even more, today there is a renewed interest for vertical axis wind turbines (VAWTs) for offshore floating arrays and wind farms with closer spacing due to their faster wake recovery [6, 7]. Aditionally, the omni-directionality of VAWTs makes them insensitive to the wind direction, resulting in a simpler mechanical design with a few moving parts, which excludes the yawing equipment and (often) the pitching mechanism. This characteristic is considerably appreciated in offshore farm facilities, because the yawing mechanism is one of the biggest sources of failures in the horizontal wind turbines (HAWT) [8–10]: the operation and maintenance take big part of the total energy cost. Another relevant advantage in VAWTs, is the fact that the generator can be placed at sea level, which stabilizes the structure due to its low center of gravity and therefore could reduce the size and cost of the floating base. Consequently, generators with larger dimensions and weight can be used, which allows for heavy direct drive generators with permanent magnets [11]. Compared to HAWTs, VAWTs have higher potential for scalability [12, 13].

VAWTs are characterized by complex and unsteady three-dimensional aerodynamics which present considerable challenges for both simulations and measurements to describe it. The near-wake structure of a VAWT has been revealed to be mainly dominated by the effects of the blade tip vortex, which produces levels of recovery (due to the vertical advection) considerably higher than those from turbulent variations [14]. This effect is not present in HAWT wakes. The energy conversion process in VAWTs is based on the variation of the blade's circulation along the rotation axis of the turbine, producing a different creation of the wake compared to HAWTs, in which the wake is only generated by the tip vortices. In order to understand the performance of VAWTs better, it is necessary to have a fundamental knowledge about the flow phenomena involved. Moreover, to maximize the efficiency of a singular VAWT within a wind farm facility, an accurate prediction of the resulting flow from an operating VAWT is essentially required. For this goal, numerical simulations can contribute useful qualitative and quantitative understanding of VAWTs wakes in a relatively fast and economical way.

The numerical works that have been carried out to investigate wakes behind VAWTs can be separated into two principal approaches. The first one consists in the full resolution of the boundary layers around the blades [15–18]. Through this method it is possible to obtain detailed information about the load distribution and the flow fields within the rotor and near wake regions. However, there is a considerable computational cost inherently involved, which restricts its utilization for wake studies in realistic large scale environments. Additionally, the accuracy of the results is directly related to the numerical method and the applied turbulence model [19, 20]. In the second approach, the blades are simulated by using the actuator type technique, which excludes the need of the full resolution of the boundary layer flow around the blade. Therefore, these simplifications makes it feasible to run studies of the far wake of VAWTs and VAWT wind farms [4, 5, 21, 22].

The present work aims to simulate the produced wake from a VAWT applying an actuator line model (ALM), and also to identify the effects of the interaction between the wake structure and the incident flow. Different terrains with their own aerodynamic roughness length have been considered. A turbulent inflow generator was not used, in order to isolate the effect of wind shear from that of turbulence intensity. The model has been implemented using the open-source CFD toolbox library OpenFOAM to solve the governing equations and to compute the resulting wake [23]. An operational H-shaped VAWT model was tested, for which experimental activity has been performed at an open site north of Uppsala-Sweden [24]. Numerical results were compared to normal forces from experimental data.

2. Methodology

An actuator line model (ALM) coupled to a dynamic stall model (DSM) has been implemented to solve the governing equation of the involved phenomena. The ALM samples the velocity from the Navier-Stokes solver, and then it calculates the angle of attack and relative velocity in each blade element. The DSM computes blade force coefficients, which the ALM uses to impart back the body force into the flow field solver. The main characteristics of the model were described in this section, it is suggested to read [25, 26] for more detailed information.

2.1. Actuator Line Model

The applied ALM is a three-dimensional and unsteady aerodynamics model developed by Sørensen and Shen [27], and created to study the surrounded flow of wind turbines. It is a coupling between a Navier-Stokes solver for the flow field with the actuator line technique, which distributes body force along lines representing the blades of the turbine. The used forces are determined through the DSM, based on empirical data.

2.2. Dynamic Stall Modeling

The DSM is represented by the Leishman and Beddoes model [28], with the variation of Sheng et al. [29] and Dyachuk [26]. It is able to compute the unsteady lift, pithing moment and drag, giving a physical description of the aerodynamics. It has been validated with experimental results in [30]. A division of three subsystems is considered in the model: an attached flow model for unsteady linear airloads, a separated flow model for non-linear airloads, and a dynamic stall model for the airloads induced by the leading edge vortex. In [25], the results have shown small improvements in the accuracy and agreement with experimental data compared to the results where the attached flow correction of the DSM is not included.

3. Simulation Parameters: Validation case

Experimental data from a 12 kW VAWT with diameter of 6.48 m were used to validate the model (Figure 1). This device is operating in a open site in the north of Uppsala. The measurement campaign and the obtained forces are published in [31] and [24], respectively; four load cells were used to measure forces on one blade and its support arms. Due to the lack of experimental results for the far wake of VAWTs in open sites, normal forces for a TSR of $\lambda = 3.44$ are used as the validation parameter. The chosen TSR value is close to the optimal one. Specifications of the turbine are shown in Table 1. In order to represent the results in an easier way, a rectangular coordinate system has been used with the origin placed at the base of the turbine, such that the x-axis is pointing positively in the downwind direction. Central shaft and supporting struts were included in the computation.

Figure 1. The 12 kW turbine, designed and built by the Division of Electricity at Uppsala University. The turbine is equipped with load cells used for the force measurements [31]

Table 1. Specification of the 12 kW VAWT used for validation

Number of blades	3
Turbine diameter	6.48 m
Hub height	6.0 m
Blade length	5.0 m
Airfoil profile	NACA0021
Chord length	25 cm
Blade pitch angle	2°
TSR	3.44°

The turbine described above was operating in different terrains with different surface roughness such that the velocity at the equator of the turbine ($z_\infty = 5.75$ m) is $U_\infty = 6.4$

m/s. The friction velocity U_{x*} and the equator-height mean wind speed are used on the log law in order to do this,

$$U_x = \frac{U_{x*}}{K} ln\left(\frac{z + z_0}{z_0}\right) \tag{1}$$

where z_0 is the roughness length and $K = 0.40$ is the von Kármán constant.

A uniform flow with a non-slip boundary condition for the ground (common configuration used for simulations), and logarithmic inlet velocity profiles in snow, long grass and bushes have been tested. These parameters are summarized in Table 2. Simulations were carried out with a domain considering open site boundary conditions.

Table 2. Aerodynamic roughness lengths used for the different cases

Case	Inlet velocity profile	z_0 [m]
1	uniform	-
2	logarithmic	0.0025 (snow)
3	logarithmic	0.055 (long grass)
4	logarithmic	0.55 (bushes)

Figure 2 displays the main characteristics of the calculated mean wind shears over the different surface types. These fields were used as incoming flows for the simulations of the resulting wake.

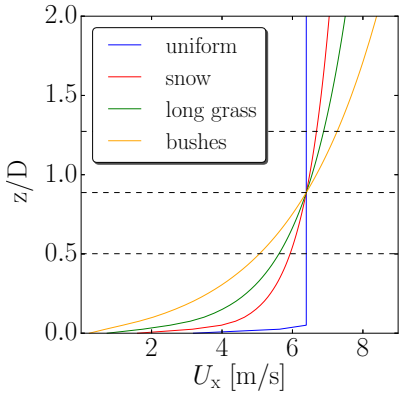

Figure 2. Vertical profiles of the streamwise velocity used at the inlet of the domain. Dashed lines represent the extent and center of the turbine

4. Results and discussion

In this section, streamwise velocity for representative planes are analyzed in order to study the wake behind the operating VAWT over the flat surfaces with different roughness lengths. The obtained normal forces were compared to experimental data. A LES Smagorinsky model has been used to predict the turbulence effects.

4.1. Mesh sensitivity

A reference mesh topology with local refinement around the region close to the turbine and in the downwind direction (in order to capture details of the obtained wake) has been used to

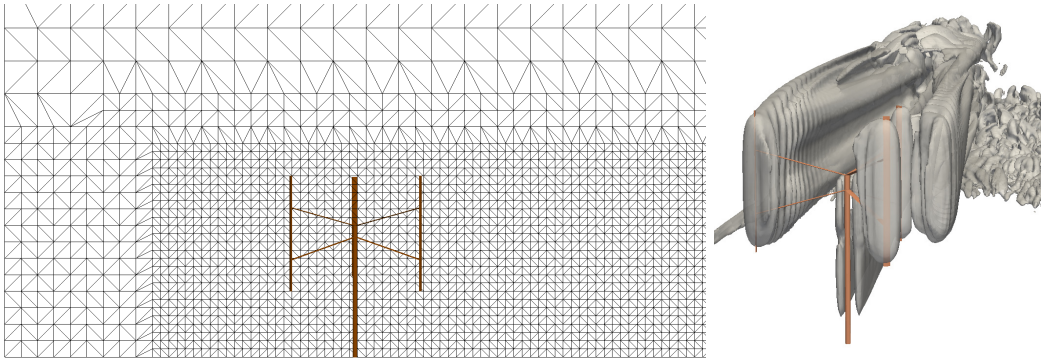

Figure 3. Illustration of the reference mesh section used with 0.43×10^6 cells (left) and vorticity isosurfaces generated by the operating turbine using 3.30×10^6 cells (right)

study the mesh sensitivity of the model, see Figure 3. This topology was kept constant and proportionally scaled in every direction for the refinements.

Figure 4 shows the normal force response during one revolution for both experimental and simulated values, varying the number of mesh points of the domain. All simulations were performed for 40 turbine revolutions to ensure convergence of the results. The surface roughness length used is $z_0 = 0.025$ m, which corresponds to the terrain of the open site where the turbine is placed. It should be noticed that there is no considerable improvement in the force predictions when increasing the mesh resolution beyond 3.3×10^6 mesh cells. Generally, the simulated results are in good agreement with the experimental values.

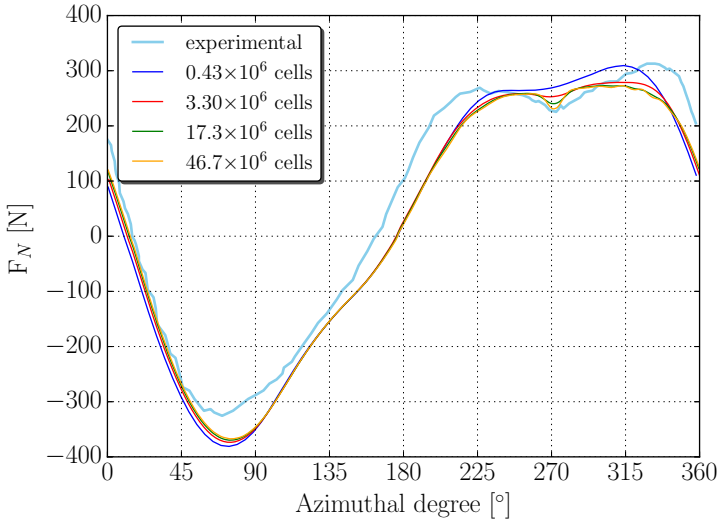

Figure 4. The normal force response for different mesh sizes

Figure 5 depicts the simulated instantaneous streamwise velocity components in the vertical plane for four different mesh sizes: 0.43, 3.3, 17.3 and 46.7×10^6 cells, which correspond to a cell size/blade-span ratio of 0.075, 0.375, 0.0213 and 0.0152, respectively. The two coarsest meshes do not have enough resolution to capture the vortical structures produced by the blade tips and the turbulent regime is not fully developed until the end of the domain. Figure 6 shows for all the cases,that the resulting wake has similar shape and position; hence the model is able

to represent the global structure of the wake independently of the mesh size. However, the refinement is necessary to capture the details of the generated vortex which has an essential contribution to the wake recovery. The wake transition to the turbulent regime is closer to the upwind direction when the mesh is finer: at x/D $\simeq$ 12 and 8 for the meshes of 17.3 and 46.7$\times 10^6$ cells, respectively.

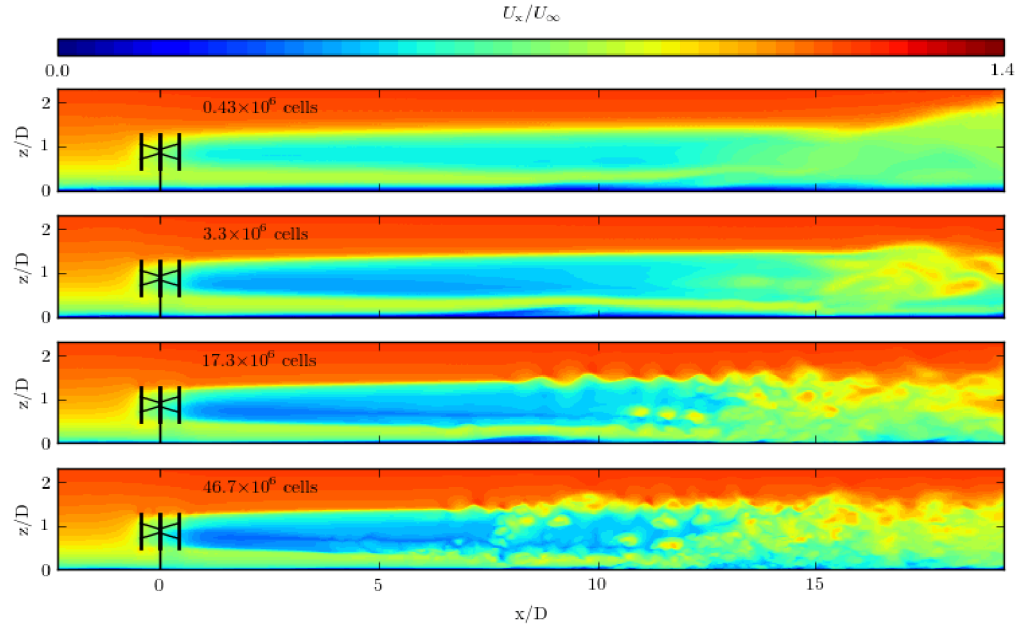

Figure 5. Normalized instantaneous streamwise velocity in the vertical plane at the centre of the turbine for different mesh sizes: 0.43, 3.3, 17.3 and 46.7$\times 10^6$ cells

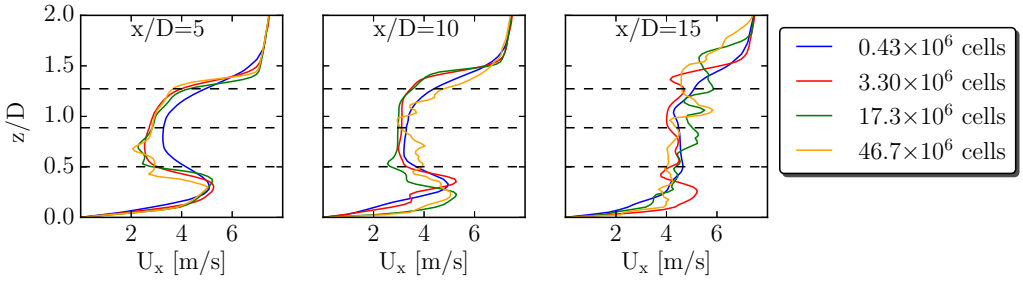

Figure 6. Vertical profiles of the instantaneous streamwise velocity component for different mesh sizes: 0.43, 3.3, 17.3 and 46.7$\times 10^6$ cells. Dashed lines represent the extent and center of the turbine

Regarding to the temporal discretization, previous studies have shown that the model is less sensitive to temporal than spacial discretization [25, 32]. Nonetheless, the Courant-Friedrichs-Lewy (CFL) condition must be taken in account for the time discretization, to ensure convergence.

4.2. Terrain roughness variation

Figures 7 and 8 reveal the resulting wake produced by the turbine. These results were obtained using a mesh resolution of 17.3×10^6 cells. In all the cases the wake shape (geometry) and position are similar. Furthermore, expansion and recovery of the wake in the downwind direction is clearly identified, as well as the uniform and logarithmic profiles at the inlet of the domain. In the vertical plane of velocity (Figure 7), it is shown that the flow is accelerated in the upper part of the wake after facing the turbine. For the uniform flow, an acceleration is also observed in the lower part of the wake. The general characteristics are mainly dominated by the vortical structures from the blade tips and the blade pitching. It could be noticed in Figure 8 that there is strong creation of vortical structures in the interface between the resulting wake and the ground and, as expected, the rougher the surface the larger turbulence. Inside the wake there is a region with no vorticity, and this becomes smaller when the surface roughness increases, which means that the wake breaks earlier to the turbulent regime. In general, larger turbulence levels lead to faster wake recovery because of the improvement of the mixing process and momentum transfer.

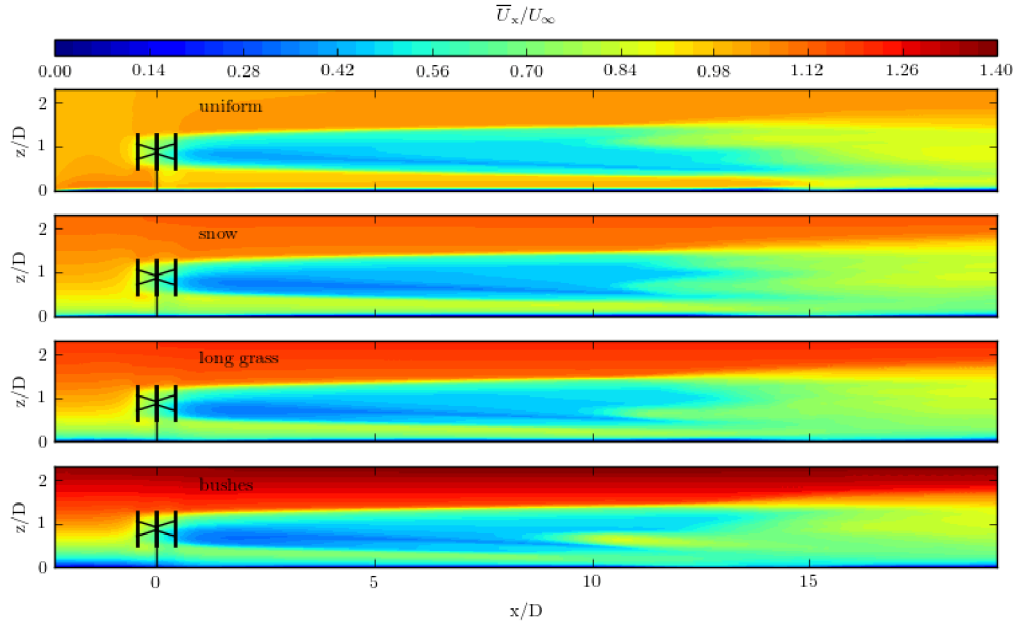

Figure 7. Normalized time-averaged streamwise velocity in the vertical plane at the centre of the turbine for different terrains: uniform flow, snow, long grass and bushes

In order to distinguish quantitatively the resulting wake structure from the different results, both horizontal and vertical profiles of normalized velocity deficit ($\triangle\overline{U}_x/U_\infty$) inside the wake region are revealed in Figure 9 for the same representative sections, where $\triangle\overline{U}_x = \overline{U}_x - U_{\text{inflow}}$ is the time-averaged velocity deficit, and U_{inflow} is the mean streamwise inflow velocity shown in Figure 2. As can be observed, the wake has a slight asymmetry in the horizontal direction, and a strong influence from the ground in the vertical structure. No significant changes are noticed until the section x/D = 10. After this, the velocity deficit decreases approximately from 50% to 30% in the equatorial area at x/D = 15. Effects leaded from the wind shears are mainly in the perpendicular direction to the main flow.

Figure 10 displays the vertical contour of the streamwise turbulence intensity for the different terrains. An evident production of turbulence intensity is noticed after the section x/D = 10,

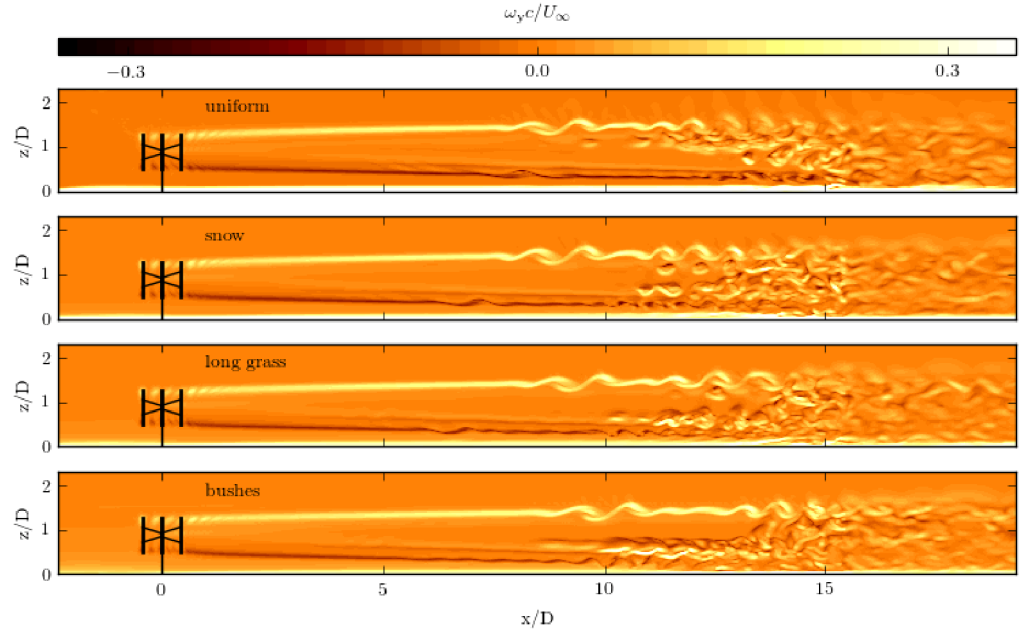

Figure 8. Normalized instantaneous cross-stream vorticity in the vertical plane at the centre of the turbine for different terrains: uniform flow, snow, long grass and bushes

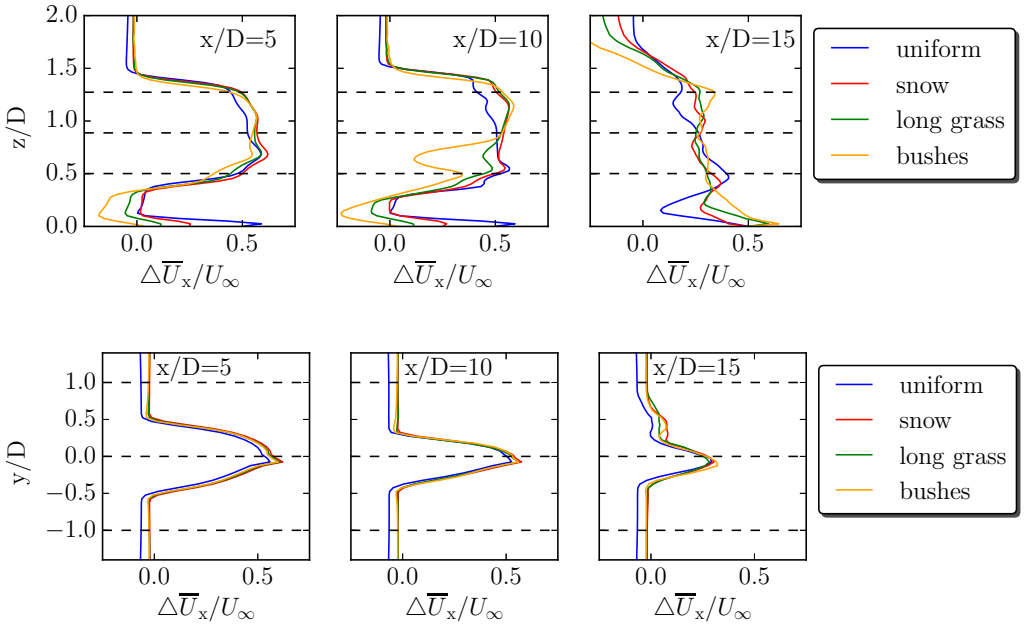

Figure 9. Vertical (up) and horizontal (down) profiles of the normalized velocity deficit for different terrains: uniform flow, snow, long grass and bushes. Dashed lines represent the extent and center of the turbine

with a higher intensity in the lower part of the wake where the shear is stronger (except for the uniform flow case). Turbulence intensity generated from the tip vortices can also be observed.

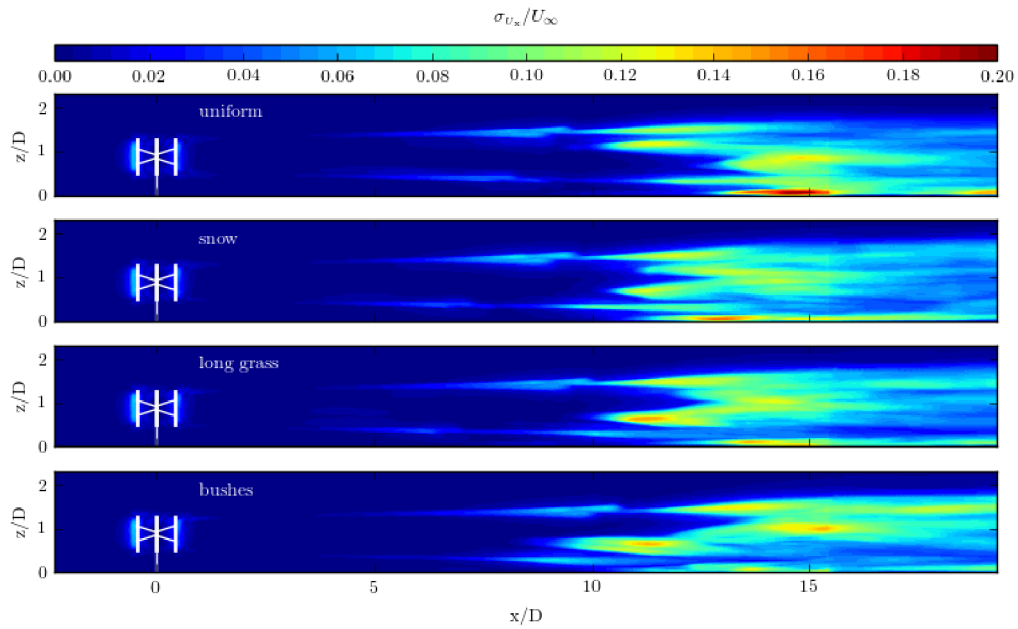

Figure 10. Streamwise turbulence intensity in the vertical plane for different terrains: uniform flow, snow, long grass and bushes

5. Conclusions

The presented ALM is able to reproduce the main pattern of a wake produced by an operating VAWT in an open site, revealing its shape and position. The numerical results showed reasonable agreement with experimental results of normal forces. The model allows to evaluate qualitatively and quantitatively the most relevant parameters and phenomenas involved in the flow pattern: velocity field with its zones of acceleration and deceleration, regions with high and low concentration of vorticity and turbulence production. Interaction between the wake and the ground is captured. Effects on the contribution from the wind shears in the mixing process and the transition to turbulent regime are clearly identified for the terrain roughness variation. The model shows stability for the tested cases, which makes it suitable for application in VAWTs simulations.

Acknowledgment

This work was conducted within StandUp for Wind, a part of the StandUp for Energy strategic research framework. The computational works were performed on resources provided by the Swedish National Infrastructure for Computing (SNIC) at NSC.

References

[1] Erik L P, Niels G M, Lars L, Jørgen H, and Helmut P F. Wind power meteorology. part i: climate and turbulence. *Wind Energy*, 1(S1):25–45, 1998.

[2] Vermeer L J, Sørensen J N, and Crespo A. Wind turbine wake aerodynamics. *Progress in aerospace sciences*, 39(6):467–510, 2003.

[3] Baidya Roy S, Pacala S W, and Walko R L. Can large wind farms affect local meteorology? *Journal of Geophysical Research: Atmospheres*, 109(D19), 2004.

[4] Shamsoddin S and Porté-Agel F. A large-eddy simulation study of vertical axis wind turbine wakes in the atmospheric boundary layer. *Energies*, 9(5):366, 2016.

[5] Abkar M and Dabiri J O. Self-similarity and flow characteristics of vertical-axis wind turbine wakes: an les study. *Journal of Turbulence*, 18(4):373–389, 2017.
[6] Dabiri J O. Potential order-of-magnitude enhancement of wind farm power density via counter-rotating vertical-axis wind turbine arrays. *Journal of renewable and sustainable energy*, 3(4):043104, 2011.
[7] Kinzel M, Mulligan Q, and Dabiri J O. Energy exchange in an array of vertical-axis wind turbines. *Journal of Turbulence*, 13(1):N38, 2012.
[8] Ribrant J and Bertling L. Survey of failures in wind power systems with focus on swedish wind power plants during 1997-2005. In *Power Engineering Society General Meeting, 2007. IEEE*, pages 1–8. IEEE, 2007.
[9] Tavner P J, Xiang J, and Spinato F. Reliability analysis for wind turbines. *Wind Energy*, 10(1):1–18, 2007.
[10] Arabian-Hoseynabadi H, Oraee H, and Tavner P J. Failure modes and effects analysis (fmea) for wind turbines. *International Journal of Electrical Power & Energy Systems*, 32(7):817–824, 2010.
[11] Eriksson S, Solum A, Leijon M, and Bernhoff H. Simulations and experiments on a 12kw direct driven pm synchronous generator for wind power. *Renewable Energy*, 33(4):674–681, 2008.
[12] Musgrove P J. Wind energy conversion: recent progress and future prospects. *Solar & wind technology*, 4(1):37–49, 1987.
[13] Peace S. Another approach to wind: vertical-axis turbines may avoid the limitations of today's standard propeller-like machines. *Mechanical Engineering-CIME*, 126(6):28–32, 2004.
[14] Bachant P and Wosnik M. Characterising the near-wake of a cross-flow turbine. *Journal of Turbulence*, 16(4):392–410, 2015.
[15] Castelli M R, Englaro A, and Benini E. The darrieus wind turbine: Proposal for a new performance prediction model based on cfd. *Energy*, 36(8):4919–4934, 2011.
[16] Bremseth J and Duraisamy K. Computational analysis of vertical axis wind turbine arrays. *Theoretical and Computational Fluid Dynamics*, 30(5):387–401, 2016.
[17] Marsh P, Ranmuthugala D, Penesis I, and Thomas G. Three-dimensional numerical simulations of straight-bladed vertical axis tidal turbines investigating power output, torque ripple and mounting forces. *Renewable Energy*, 83:67–77, 2015.
[18] Posa A, Parker C M, Leftwich M C, and Balaras E. Wake structure of a single vertical axis wind turbine. *International Journal of Heat and Fluid Flow*, 61:75–84, 2016.
[19] Lam H F and Peng H Y. Study of wake characteristics of a vertical axis wind turbine by two-and three-dimensional computational fluid dynamics simulations. *Renewable Energy*, 90:386–398, 2016.
[20] Chowdhury A M, Akimoto H, and Hara Y. Comparative cfd analysis of vertical axis wind turbine in upright and tilted configuration. *Renewable Energy*, 85:327–337, 2016.
[21] Pierce B, Moin P, and Dabiri J. Evaluation of drag forcing models for vertical axis wind turbine farms. In *APS Meeting Abstracts*, November 2013.
[22] Shamsoddin S and Porté-Agel F. Large eddy simulation of vertical axis wind turbine wakes. *Energies*, 7(2):890–912, 2014.
[23] Bachant P, Goude A, and W Martin. turbinesFoam: v0.0.7. Zenodo. http://dx.doi.org/10.5281/zenodo.49422, 2016.
[24] Dyachuk E, Rossander M, Goude A, and Bernhoff H. Measurements of the aerodynamic normal forces on a 12-kw straight-bladed vertical axis wind turbine. *Energies*, 8(8):8482–8496, 2015.
[25] Mendoza V, Bachant P, Wosnik M, and Goude A. Validation of an actuator line model coupled to a dynamic stall model for pitching motions characteristic to vertical axis turbines. In *Journal of Physics: Conference Series*, volume 753, page 022043. IOP Publishing, 2016.
[26] Dyachuk E. *Aerodynamics of vertical axis wind turbines: Development of simulation tools and experiments*. PhD thesis, Acta Universitatis Upsaliensis, 2015.
[27] *Computation of Wind Turbine Wakes using Combined Navier-Stokes/Actuator-line Methodology*.
[28] Leishman J G and Beddoes T S. A generalised model for airfoil unsteady aerodynamic behaviour and dynamic stall using the indicial method. In *Proceedings of the 42nd Annual forum of the American Helicopter Society*, pages 243–265. Washington DC, 1986.
[29] Sheng W, Galbraith R A, and Coton F N. A modified dynamic stall model for low mach numbers. *Journal of Solar Energy Engineering*, 130(3):031013, 2008.
[30] Leishman J G and Beddoes T S. A semi-empirical model for dynamic stall. *Journal of the American Helicopter society*, 34(3):3–17, 1989.
[31] Rossander M, Dyachuk E, Apelfröjd S, Trolin K, Goude A, Bernhoff H, and Eriksson S. Evaluation of a blade force measurement system for a vertical axis wind turbine using load cells. *Energies*, 8(6):5973–5996, 2015.
[32] Bachant P, Goude A, and Wosnik M. Actuator line modeling of vertical-axis turbines. *arXiv preprint arXiv:1605.01449, Submitted to Wind Energy*, 2016.